J. Membrane Biol. 146, 73–84 (1995)

The Journal of
Membrane
Biology

Voltage-dependent Sodium Currents Recorded from Dissociated Rat Taste Cells

M.S. Herness, X.-D. Sun
Indiana University School of Medicine, Center for Medical Education, Ball State University, Muncie, IN 47306

Received: 31 October 1994/Revised: 28 February 1995

Abstract. Voltage-dependent sodium currents were analyzed in detail from dissociated mammalian taste receptor cells using the whole-cell patch clamp technique. Approximately 50–75% of all taste receptor cells expressed sodium currents. These currents activated close to −50 mV (holding potential = −80 mV) with maximal currents most often occurring at −10 mV. The distribution of maximal inward currents across all cells appeared to display two peaks, at −254 pA and −477 pA, possibly due to differences in sodium channel density. Inward currents were eliminated by replacing 90% of external sodium with N-methyl-D-glucamine. The current-voltage relationship of the activated current, as measured by a tail current analysis, was linear, suggesting an ohmic nature of the open channel conductance. The relationship between the time to the peak activated current and the step potential was well fit by a double exponential curve (τ_1 = 6.18, τ_2 = 37.8 msec). Development of inactivation of the sodium current was dependent upon both voltage- and temporal-parameters. The voltage dependence of the time constant (τ) obtained from removal of inactivation, development of inactivation, and decay of the sodium current displayed a bell-shaped curve with a maximum of 55 msec at −70 mV. In addition to fast inactivation (half maximal at −50 mV), these currents also displayed a slow inactivation (half maximal at −65 mV). Voltage-dependent sodium currents were reversibly inhibited by nanomolar concentrations of tetrodotoxin ($K_d = 10^{-8}$ M). There was no evidence of a TTX-insensitive sodium current. This description broadens our understanding of gustatory transduction mechanisms with a particular relevance to the physiological role of receptor cell action potentials.

Key words: Gustation — Taste — Sensory transduction — Sodium current — Patch clamp

Correspondence to: M.S. Herness

Introduction

Gustation is an excellent experimental choice for the study of sensory transduction since the depth of information needed to be recognized and encoded within taste stimuli is far less complicated than higher sensory systems such as vision or audition, yet the distinct sensations of salty, sour, bitter, and sweet provide accessible experimental handles for quality coding when compared to lower senses.

Taste cells are differentiated epithelial cells sequestered in morphological structures referred to as buds. A few cells within the bud form synaptic connections to the afferent neuron. Additionally, taste cells may be connected to other taste cells via gap junctions [2, 20, 41]. For many years it was thought that the taste cell relayed its signal to the afferent nerve by modulating synaptic release through a graded receptor potential, usually depolarizing. It now appears that taste cells utilize action potentials to transmit information. Action potentials were first recorded in taste cells over a decade ago [23, 36] yet their physiological role remains unclear. Patch clamp analysis of membrane currents from taste receptor cells [1, 5, 9, 27, 38] has made clear that not all taste receptor cells possess voltage-sensitive sodium currents and hence not all would be expected to propagate action potentials. Of those cells capable of active propagation a central question remains—do these cells produce action potentials to communicate with the primary afferent neurons through transmitter release, or with other taste cells, via gap junctions, or do both avenues provide routes for active informational interchange within the bud?

The voltage-sensitive sodium channel is fundamental to the propagation of the action potential by controlling the time- and voltage-dependent conductance of sodium across the cell's membrane. From detailed characterizations in a variety of preparations such as neurons, glia, skeletal and cardiac muscle, it is clear there are a

variety of voltage-dependent sodium currents which can be categorized on the basis of electrophysiological, pharmacological, biochemical, and molecular criteria. Characterization of the biophysical and pharmacological properties of these currents is required since a fair amount of heterogeneity exists in describing features of sodium currents from differing cell types.

Though a few records of sodium currents from mammalian taste receptor cell have been reported [1, 9, 38] only one [9] has offered a preliminary analysis of these currents, though it was not the major focus of the study. Much of the biophysical characterization of sodium currents in mammalian taste receptor cells, such as the distribution of the maximal inward currents, a more complete description of the influence of voltage and temporal parameters on the time constants of the inactivating current, the presence of slow inactivation, and the dose-response relationship of TTX sensitivity are still lacking. These are essential to a comprehensive description of taste transduction mechanisms. This paper sets out to characterize in detail electrophysiological properties of sodium currents from these cells.

Materials and Methods

Voltage-dependent sodium currents were recorded from isolated rat taste receptor cells that were voltage-clamped using patch clamp recording techniques in the whole cell configuration.

Dissociation Procedure

Isolated rat taste receptor cells were obtained as previously described [18]. Circumvallate or foliate papillae were chosen for dissociation due to their high density of taste buds. Moreover, sodium currents have not been described from posterior cells. These papillae were excised from an anesthetized Sprague-Dawley male rat (0.09 ml/100 gm BW Ketamine (91 mg/ml; Fort Dodge Laboratories) and Acepromazine (0.09 mg/ml; Butler Laboratories) mixture). Excised tissue was incubated in a cysteine-activated (1 mg/ml) Papain/divalent-free bicarbonate-buffered solution (14 U/ml) for two hours at 32°C in 5% CO_2/95% Air. After incubation, the tissue block was transferred to a pseudo-extracellular fluid (ECF) and the epithelium removed with fine forceps releasing dissociated gustatory and nongustatory cells. Some papillae were maintained in an ice-cold ECF solution for later dissociation. Taste cells were conclusively identified from other lingual cells by their characteristic morphology. Cells remained viable for hours after dissociation as evidenced by the absence of membrane blebs and the quality of voltage-clamp recording conditions.

Solutions

Pipettes were filled with a pseudo-intracellular solution composed of (mM): 140 KCl, 2 Mg_2Cl, 1 $CaCl_2$, 11 EGTA, 10 Na HEPES, and 10 4-AP (free $[Ca^{++}]$ of 10^{-8} M) and adjusted to pH 7.2 with KOH. In later experiments 4 mM ATP (disodium salt, Na_2ATP) was also included with HEPES adjusted (2 mM Na HEPES, 8 mM HEPES) so that pipette concentration of sodium remained at 10 mM.

The divalent-free solution for enzymatic incubation was composed of (mM): 65 NaCl, 20 KCl, 26 $NaHCO_3$, 2.5 $NaH_2PO_4 \cdot H_2O$, 20 D-glucose, 1 EDTA, and phenol red (2 µl/ml). This solution maintains a pH of 7.2 to 7.4 in a 5% CO_2 incubator. The composition of the ECF solution was (in mM): 126 NaCl, 5 KCl, 2 $CaCl_2$, 2 $MgCl_2$, 5 Na HEPES, 1.25 $NaH_2PO_4 \cdot H_2O$, 10 D-glucose, 20 TEA, and 0.5 $CdCl_2$. ECF was adjusted to pH 7.4. In experiments where extracellular sodium was replaced with N-methyl-D-glucamine (NMDG; 90% Na-free) the ECF composition was (in mM): 8.1 NaCl, 117.9 NMDG, 5 KCl, 2 $CaCl_2$, 2 $MgCl_2$, 5 Na HEPES, 10 D-glucose, 20 TEA, and 0.5 $CdCl_2$.

Data Acquisition and Analysis—Whole Cell Recordings

Data were acquired with a commercially available set of acquisition/analysis software (pClamp; Axon Instruments) using a 386 or 486 based computer, a LABMASTER DMA daughter board (Scientific Solutions, 125 kHz throughput), and an Axopatch 1B or Axopatch 200A amplifier (Axon Instruments). All recordings were obtained at room temperature, typically 22°C.

Glass (potash soda lead, Dagan Corporation; or borosilicate, W.P.I.) micropipettes were manufactured with multiple stages on a microprocessor controlled gas jet puller (Sutter Instruments). Electrode resistances were typically 3–4 MΩ when filled with pseudo-intracellular solution and measured in ECF. Neither Sylgard coating nor fire polishing of micropipette tips proved necessary. Gigaseals were formed by application of slight negative pressure to the pipette interior; resistances were often in excess of 20 GΩ. Fast capacity transients associated with stray capacity to ground were compensated. Slow capacity compensation was employed as necessary. The settling time of capacitive transients was 131 µsec (±3 µsec, n = 93 cells) when filtered at 10 kHz. After rupture of the membrane patch occluding the electrode tip, compensation of the whole cell membrane capacitance and measurement of the series resistance was employed. Whole cell membrane capacitance was taken as the magnitude of the whole cell compensation dial and was typically 3 to 6 pF. Assuming the taste cell to be an ellipsoid (major axis a = 25µ; minor axis b = 2.5µ) rotated about its major axis one can calculate the surface area from the formula $SA = 2\pi b^2 + 2\pi ab/e \arcsin(e)$ where e is the eccentricity $e = \sqrt{a^2 - b^2}/a$. This produces a value of 615µ^2 for a cell 50µ long that is 5µ at its widest. Dividing total measured membrane capacitance by the estimated surface area produces a specific membrane capacitance of 0.976 µF/cm^2, a value in good agreement with the usual 1 µF/cm^2, considering the approximate nature of the surface area. Uncompensated series resistance was taken as the series resistance setting of the amplifier that produced optimal transient balancing. It averaged 10 MΩ.

Voltage protocols were generated by the software driven D/A converter. Typically, cells were held at −80 mV and the membrane potential was stepped to voltages ranging from −100 to +80 mV in 10 mV increments applied for 8 msec duration. Membrane potential was held at −80 mV between trials. The whole-cell records obtained were the average of three successive runs. Other protocols, e.g., in measuring voltage dependence of inactivation, are described in Results.

Signals were low pass filtered with a four-pole Bessel filter (80 dB per decade) with a cut off (−3 dB) frequency of 10 kHz. Currents were sampled approximately every 19.5 µsec. An online leak subtraction protocol was employed that partitioned the inverted amplitude of the command pulse over four subpulses prior to the command pulse at 10 msec intervals with a 20 msec settling time separating delivery of

the subpulses from the command pulse. Only leak subtracted traces were stored for further analysis. Low-pass resistance-capacitance (*R-C*) filtering in the whole-cell recordings (due to the remaining series resistance and the cell capacitance) was considered minimal. On the average the product of the remaining series resistance and the cell capacitance gave a time constant average (τ) of about 37 μsec. This gives a cut-off frequency ($f_c = 1/2\pi RC$) of about 4.3 kHz.

Data were analyzed with a combination of offline software programs that included commercially available analysis programs (Clampan, Clampfit, Axon Instruments, CA), as well as data export to either a spreadsheet program (Excel, Microsoft, WA) and/or a technical graphics/analysis program (Origin, MicroCal Software, MA).

Results

Sodium Currents

Transient inward currents were recorded in many but not all dissociated taste receptor cells when the membrane potential was stepped sufficiently positive to its holding level. This current activated rapidly then more slowly declined towards zero, although the membrane voltage was maintained at the more positive potential. If the membrane potential was stepped to very positive potentials (e.g., > +60 mV), this transient current was recorded as an outward current that maintained similar, if not slightly accelerated, temporal characteristics. These currents are thought to be carried by sodium ions since they displayed voltage, temporal, and inactivation characteristics consistent with voltage-dependent sodium currents from other cells, their inward components disappeared with removal of external sodium ion, they reversed at very near predicted values for the sodium equilibrium potential, and they were sensitive to the classic sodium channel blocker tetrodotoxin.

Figure 1 shows typical sodium currents obtained from a dissociated taste receptor cell. From a holding potential of −80 mV, currents were first detectable at steps to −40 mV and reached a peak inward value at −10 mV. A reversal potential of 51 mV corresponded reasonably well with the sodium equilibrium potential, E_{Na}, calculated from the known concentrations of external Na^+ and estimated internal concentration. From the *I-V* curve the first phase of the curve reaches a half maximum of approximately −25 mV and a peak inward current of −493 pA occurs at −10 mV.

To confirm that these currents are carried by sodium, they were recorded in a bath solution in which most of the extracellular sodium had been replaced by the nonpermeant cation; N-methyl-D-glucamine, (NMDG-ECF). As illustrated in Fig. 2*A*, currents measured in NMDG-ECF were absent of inward components though outward currents were maintained by internal sodium. The elimination of the inward currents was reversible

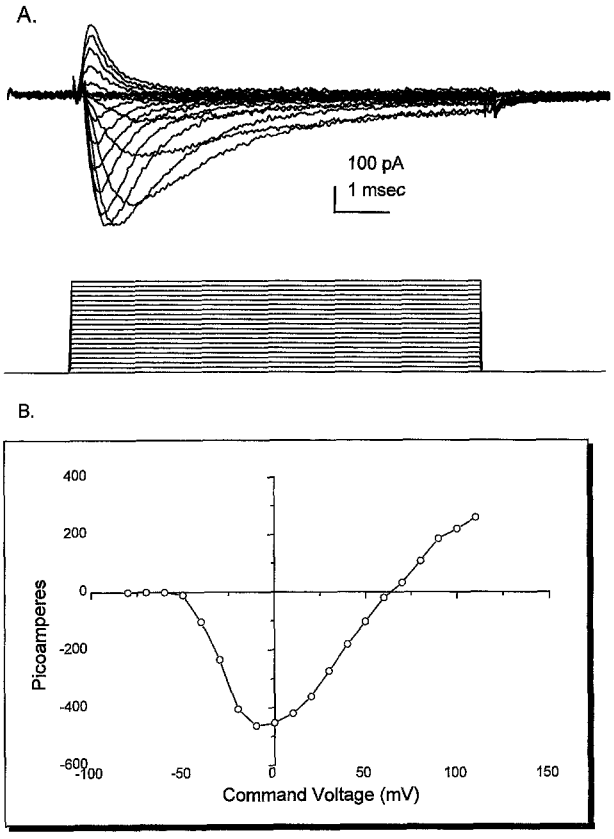

Fig. 1. A representative family of voltage-dependent sodium currents (*A*) recorded from a dissociated taste receptor cell. Currents were evoked by 10 mV incremental step potentials from a holding potential of −80 mV to a final step of +110 mV. Illustrated traces were offline filtered with a time constant of 500 μsec. In (*B*) the peak current magnitudes are plotted against their corresponding step potential. Activation of current was detected at approximately −50 mV. A maximal inward current of −463 pA occurred at −10 mV and the current became outward at potentials positive to 60 millivolts.

when NMDG-ECF was replaced with ECF. The current-voltage relationship in the two extracellular solutions is presented in Fig. 2*B* as mean values with standard error (n = 7). The reversal potential in NMDG-ECF shifted to the left from a value of 55 mV to a value between 0 and 10 mV. This agrees reasonable well with a value of 7 mV predicted by the Nernst equation with an internal concentration of 10 mM sodium and external sodium concentration of 13.1 mM.

Activation Properties of I_{Na}

The activation of the sodium conductance was highly voltage-dependent. The sodium conductance, G_{Na}, could be reasonably estimated at a series of membrane potentials, E_m, according to the relationship:

$$G_{Na} = I_{Na}/(E_m - E_{rev}) \quad (1)$$

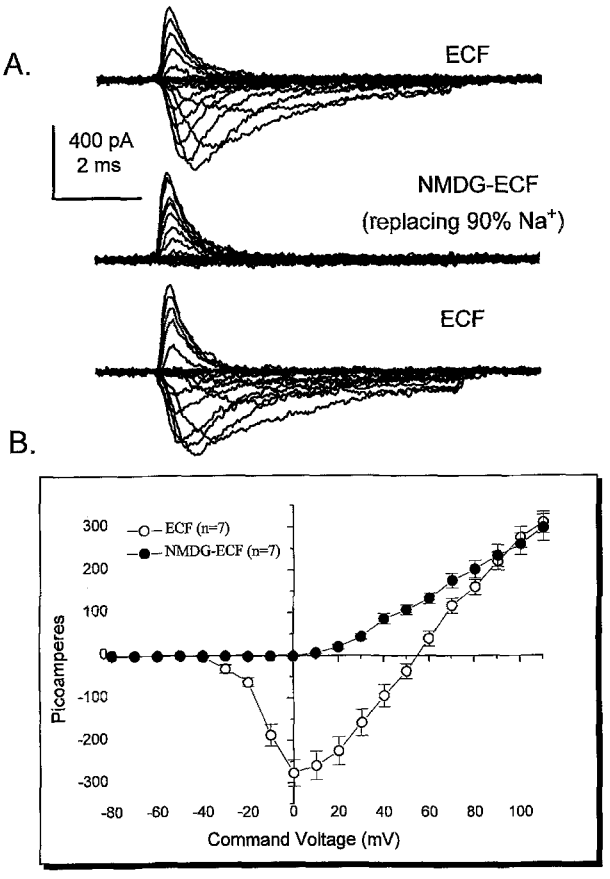

Fig. 2. In (*A*) a family of sodium currents, elicited by the same voltage protocol as in Fig. 1, is illustrated in the presence of the usual bath solution containing 131 mM external sodium (ECF) or one in which 90% of the external sodium has been replaced by the nonpermeant cation N-methyl-D-glucamine (NMDG-ECF). The current-voltage relationship for seven cells (mean ± SEM) is plotted in (*B*) for ECF or NMDG-ECF. The shift to the left of the reversal potential is very close to predicted values from the Nernst equation.

using empirically derived values for the sodium current, I_{Na}, and for the reversal potential, E_{rev}. The voltage dependence of the sodium conductance from a representative taste cell is illustrated in Fig. 3*A* (current traces are shown in the inset). Data were fitted with an equation of the form:

$$G_{Na} = G_{max}/\{1 + \exp((E_{1/2} - E_m)/a_g)\}, \quad (2)$$

where G_{max} is the maximum conductance, $E_{1/2}$ is the potential at half maximal conductance, E_m is the membrane potential and a_g is the steepness coefficient and is equal to kT/ze (where k is Boltzman's constant, T is absolute temperature, e is the elementary charge, and z is the equivalent charge of the gating particle if the transition of the channel from a nonconducting to a conducting state involved this particle moving across the entire membrane field). For this cell, conductance was half maximal at −24 mV and the steepness coefficient, a_g, was 6.6 mV/e-fold. At potentials more positive than about +40 mV there was a gradual and increasing reduction of the sodium conductance that was observed in all experiments. This decline in conductance at very positive potentials has been noted by others in muscle [4, 33], glia [8, 21], and brain sodium channels expressed in oocytes [39]. In these preparations, this decline is evident whether the data are plotted as conductance, g, or as the sodium permeability coefficient from the constant field relationship, P_{Na}. It has been ascribed to an inability of the open channel to obey the constant-field equation at these higher potentials. However, it has been noted that in the squid axon the decline in conductance at higher potentials was not evident if plotted as P_{Na} [24]. Our data followed the latter relationship; the conductance decline was not manifest if plotted as sodium permeability coefficient from the constant field relationship.

As the magnitude of the step between the holding to command potential increased (and hence the change in voltage with respect to time, dV/dt, increased) the onset temporal patterns of these currents became more abrupt. The voltage dependence of the time-to-peak current is illustrated in Fig. 3*B*. The magnitude was largest, 2 to 3 milliseconds, for near threshold depolarizations (e.g., −50 to −40 mV) and asymptotically decreased to less than one-half millisecond. Time-to-peak data could be adequately described by a single exponential decay function with a time constant of 21.7 msec. The short time-to-peak values observed from these cells (0.44 msec ± 0.02 SEM., n = 28) may be attributed, at least in part, to a careful minimization of the series resistance, R_{ser}. Any increases in R_{ser} would produce longer time-to-peak values and probably decrease the maximum inward current due to slower voltage control and increased low-pass *R-C* filtering.

The potential at which the recorded current reversed from inward to outward averaged 56 mV (±0.58 SEM., n = 137 cells) and ranged from 40.5 mV to 69 mV. These values are thought physiological because exchange of sodium in the pipette solution with the cytoplasm is known to occur with a time constant of several seconds [28] and values of R_{ser} were low. When reversal potential values were tested against whole cell membrane capacitance or R_{ser}, no correlation was noted. This suggested that neither cell size nor pipette exchange was a limiting factor influencing internal sodium concentration.

Data from 137 taste receptor cells are presented in the Table. The mean value for the zero-current potential deserves special comment. One contributing factor to the apparent depolarized state of the cells (−40 mV) may be the inherent chemosensitivity of taste receptor cells. Unlike the situation *in situ*, in the dissociated state both apical and basal surfaces of the cell are exposed to the same bathing solution. Many chemoreceptors respond well to sodium and the high sodium concentration of the ECF (131 mM) would depolarize these cells. Cells in-

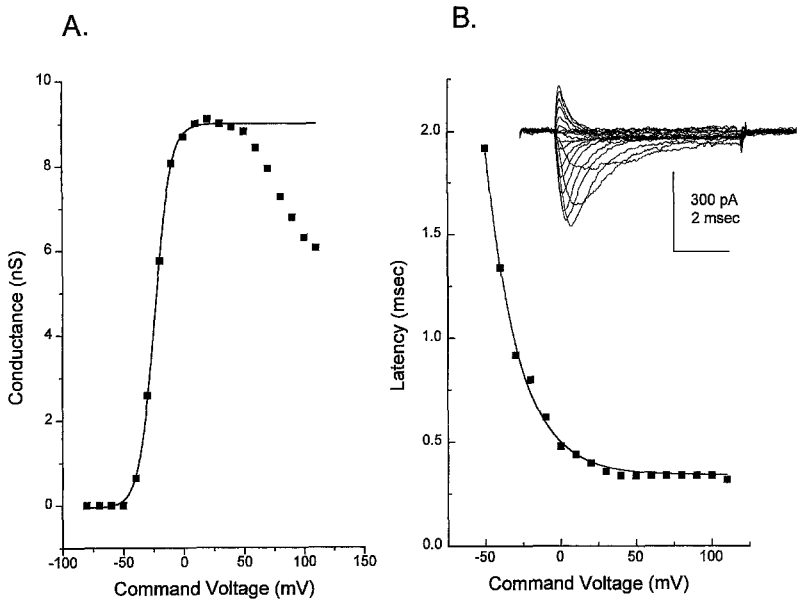

Fig. 3. The whole cell sodium conductance (■), calculated from Eq. (1), is plotted against its corresponding step potential in (*A*). The superimposed curve, calculated from Eq. (2), produced a half maximal voltage of −24 mV, a steepness coefficient of 6.6 mV/e-fold, and an asymptotic maximal conductance of 9.1 nS. The time to the peak current (*B*), from the same cell, was adequately described by a single exponential (τ = 21.7 msec) that asymptotes at 0.34 msec, a minimal latency value typical of many cells. The family of sodium currents recorded from this cell is illustrated in inset (78 μsec blanking was employed to eliminate the capacitance transients).

Table. Electrophysiological characteristics of taste receptor cells and their voltage-dependent sodium currents

		I_{zero} (mV)	I_{hold} (nA)	R_{in} (GΩ)	C_m (pF)	S_r (MΩ)	I_{max} (pA)	G_{max} (nS)	Time to peak (msec)	E_{rev} (mV)
All cells		−37.3	−0.17	3.66	3.8	9.4	−327	7.29	0.44	54.9
		± 5.1	± 0.35	± 0.41	± 0.1	± 0.8	± 16	± 0.29	± 0.02	± 1.0
		(35)	(67)	(67)	(123)	(36)	(125)	(125)	(37)	(125)
	Min	0	<−0.01	0.04	2.0	4.0	−60	0.75	0.2	8.5
	Max	−85	−2.15	8.9	10.0	21	−672	18.4	0.84	83.0
Peak 1		−30.8	−0.16	4.02	3.6	8.8	−249	5.99	0.43	55.1
		± 7.9	± 0.06	± 0.52	± 0.1	± 1.0	± 7	± 0.21	± 0.03	± 1.2
		(15)	(44)	(44)	(88)	(16)	(90)	(90)	(17)	(90)
	Min	0	<−0.01	0.04	2.0	5	−92	2.0	0.34	8.5
	Max	−85	−2.15	8.9	10.0	20	−390	10.0	0.8	83.0
Peak 2		−46.2	−0.22	3.60	3.9	10.5	−469	10.1	0.43	54.1
		± 8.6	± 0.08	± 0.94	± 0.3	± 1.5	± 8	± 0.51	± 0.04	± 2.1
		(14)	(16)	(16)	(26)	(14)	(26)	(26)	(14)	(26)
	Min	0	<−0.01	0.074	2.4	4	−400	6.1	0.2	35.3
	Max	−80	−1.07	8.0	9.0	21	−540	15.3	0.8	75.0

For each group, values are expressed as the mean ± SEM. The number of observations is given in parenthesis immediately below each value. Abbreviations are as given in text.

cluded in the study had otherwise normal characteristics (such as input resistance, peak magnitude of current, and reversal potential) suggesting adequate clamping conditions. Moreover, when the zero-current potential was measured in NMDG-ECF (90% sodium free) and compared to its value in ECF it hyperpolarized by 18.1 mV (n = 5, SE ± 2.7 mV). Hence the intrinsic sensitivity of some cells to sodium in the ECF likely contributes more to their depolarized state than extrinsic variables such as cell damage or poor clamping conditions.

Dissociated taste cells exhibited maximal inward currents that ranged from −60 pA to −672 pA (Table). Visual inspection of the distribution of maximal inward current, tabulated in 25 pA bins and presented in histogram form (Fig. 4), offered the possibility of two peaks in the ensuing pattern. A Gaussian analysis of the data is superimposed on the bins in Fig. 4; the data appear to be reasonably described by a twin peak description with a primary peak centered at −254 pA (width 160 pA) and a smaller peak at −477 pA (width 94 pA). The primary peak accounted for 83% of the area under the curves. Correlations of peak inward current with dissociation conditions or visible signs of cell damage were not observed. This analysis suggests that a nonhomogeneous

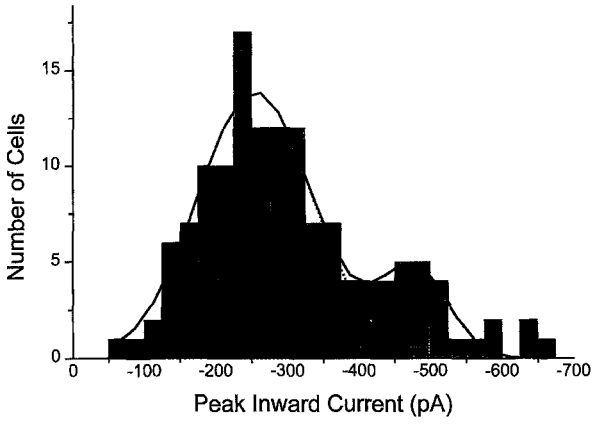

Fig. 4. The distribution of the maximal inward sodium current recorded from 137 taste receptor cells is presented in histogram form. Cells were grouped with a bin width of 25 pA. The data were fitted with a twin peak Gaussian distribution. Peaks occurred at −255 pA and at −477 pA and had widths of 160 pA and 94 pA respectively. The area beneath the first peak was approximately five times that of the second peak.

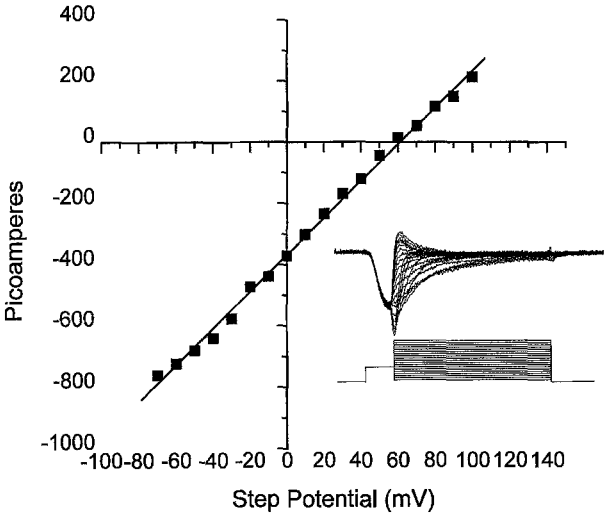

Fig. 5. The instantaneous current-voltage relationship of the voltage-dependent sodium current was tested with a two-pulse protocol. The first step elicited a near maximal inward current. After 0.5 msec, the membrane potential was abruptly changed to a variety of test potentials, plotted on the abscissa. The ensuing relationship was linear suggesting an ohmic nature to the open channel conductance. The line represents a linear regression analysis of the data points (r = 0.9984).

array of the sodium current density would be worthy of discussion.

Open Channel (Instantaneous) Current-Voltage Relationship

The assumption of ohmic linearity of the open channel conductance (i.e., the instantaneous current-voltage relationship) was tested by a two-pulse voltage protocol. The first pulse, from a holding potential of −80 mV to a command potential of −10 mV, was chosen to elicit a maximal inward current. After 0.5 msec, which approximately coincided with the peak of the maximal inward current, a second test pulse was applied to varying potentials. Current was measured as the peak of the tail current and plotted against the latter pulse potential (Fig. 5). The ensuing relationship was linear in all tested cells (n = 7). The current reversed close to an expected sodium equilibrium potential (calculated 61 mV), indicating the tails were carried by sodium. A linear regression analysis appeared to adequately describe the curve (r = 0.9984) with a calculated slope conductance of 6.0 nS. This same cells yielded a maximum conductance of 9.2 nS, which occurred at +10 mV, when tested with the voltage protocol illustrated in Fig. 1. In the large majority of recorded cells, maximum conductance occurred at membrane potentials more positive than that producing the maximum inward current.

Inactivating Sodium Current

The inactivating portion of the sodium current was measured from the peak maximal current back to the zero current level and was well fit by a single exponential relationship. An example for one current trace is illustrated in the inset of Fig. 6. The time constant describing a single current trace displayed marked voltage-sensitivity, becoming faster at more positive command potentials. The ensuing exponential relationship of command voltage *vs.* time constant (Fig. 6) was best described by a double exponential with a fast (τ_1) and a slow (τ_2) components. This suggests that underlying processes responsible for the decline in current are complex.

Voltage- and Temporal-Dependence of Inactivation

The amount of sodium current elicited by a particular voltage step can be greatly influenced by the prior history of the membrane potential since some fraction of channels have been placed in inactivated states and can no longer contribute to the macroscopic current. Voltage dependence of sodium current inactivation—termed fast inactivation (the Hodgkin-Huxley h_∞ plot)—was investigated with a typical two-pulse protocol (prepulse and test pulse) that allowed evaluation of the noninactivated fraction of the sodium current as a function of a prepulse membrane potential. Prepulses 100 msec in duration and of variable amplitude (−100 to −20 mV) were applied prior to the test pulse to −10 mV. Cells were held at −80 mV between trials. Prepulses activated little sodium current but produced noticeable inactivation as assayed by the subsequent test pulse. Data from a representative cell

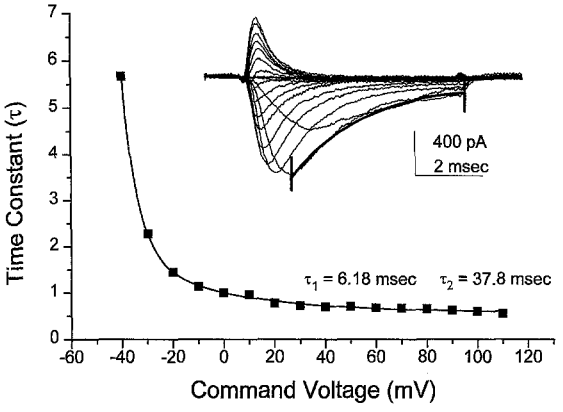

Fig. 6. The voltage dependence of the time constant for the inactivating portion of the sodium current is plotted as a function of the membrane potential. Current traces were fitted using a single exponential relationship, as illustrated in inset. The relationship between time constant and step potential was not well fitted by a single exponential relationship but was well described by a double exponential curve, as illustrated, with τ_1 = 6.18 msec and τ_2 = 37.8 msec.

are illustrated in Fig. 7. Data were well fitted by an equation of the form:

$$h_\infty = 1/\{1 + \exp((E_m - E_h)/a_h)\}, \quad (3)$$

where E_m is the membrane potential, E_h is the prepulse potential at which inactivation is half-maximal, and a_h equals kT/ze (where k, t, z, and e have the same meanings as previously described). Half-maximal value (E_h) was −55 mV in this cell and the steepness coefficient, a_h, was 5.4 mV/e-fold.

The data from a large number of cells for fast inactivation and conductance are illustrated in Fig. 8 as mean data points ± SEM. To ease comparison, data were normalized to unity. At membrane potentials more positive to −90 mV, inactivation becomes apparent (10% inactivated current at −70 mV). Half-maximal inactivation occurred at −51 mV (n = 17 cells), was essentially complete by −20 mV, and the steepness coefficient was 7.3 mV/e-fold. This half maximal value (from posterior taste cells) compares favorably with the value of −50 mV reported from two anterior taste cells in rat [9]. Both are more positive than the half-maximal value of −65 mV reported from frog taste receptor cells [5]. Inactivation of sodium currents in frog taste receptor cells was complete by −50 mV.

Macroscopic conductance of the sodium current was maximal at +10 mV; half-maximal conductance occurred at −22 mV and the steepness coefficient was 5.3 mV/e-fold. At −10 mV, where maximal sodium current was elicited, the conductance was 78% of its maximal value. A small "window" is present where the inactivation and conductance curves overlap. In the area of overlap, some channels would be activated that then would not inactivate. The peak of this window of overlap occurs at

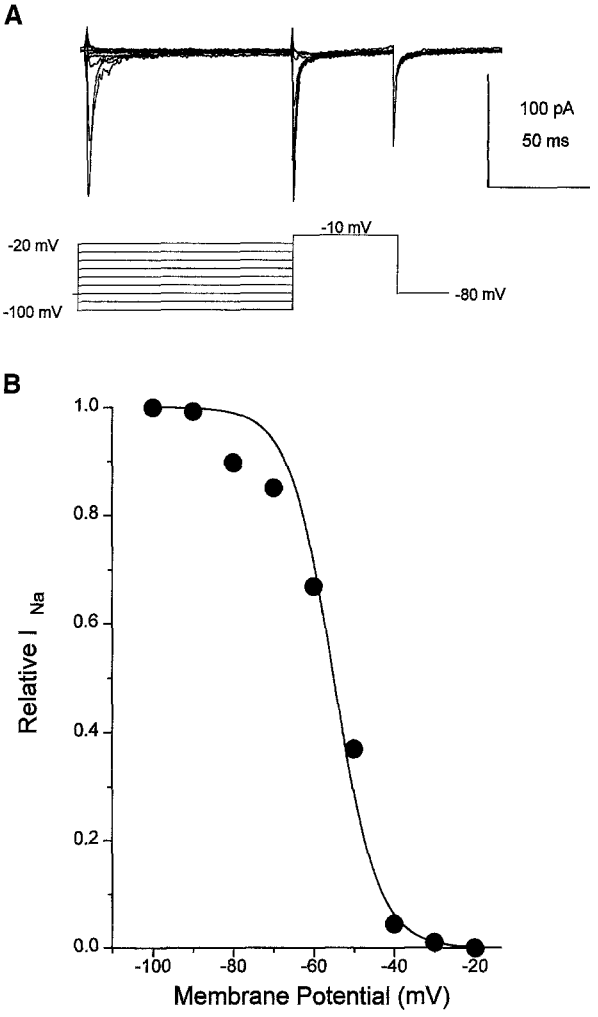

Fig. 7. The development of voltage-dependent inactivation was investigated using a two-pulse voltage protocol as illustrated in (*A*). Current magnitudes of the test pulse were normalized to its maximal value. As illustrated in (*B*), when the membrane potential became more positive than −90 mV, a measurable diminution to the test pulse occurred. The calculated half maximal voltage was −55 mV and the steepness coefficient was 5.4 mV/e-fold for this cell.

−33 mV where h_∞ = normalized g(Na) = 10% of maximal values.

In addition to fast inactivation, the phenomenon of slow inactivation (s_∞) of the sodium current could be demonstrated. If the prepulse was applied to the cell for long periods of time (5 sec) then the voltage dependence of the inactivation curve shifted to the left by approximately 15 mV. These data are displayed in Fig. 9; data for fast and slow inactivation were obtained from the same cells. There was no apparent change in the time course of the sodium currents as illustrated in the inset. The half-max value for s_∞ was −65 mV compared to −50 mV for h_∞. Steepness coefficients were 6.4 and 6.7 mV/e-fold for slow and fast respectively. The slow inactivation was complete by −40 mV.

A more detailed analysis of the inactivation time

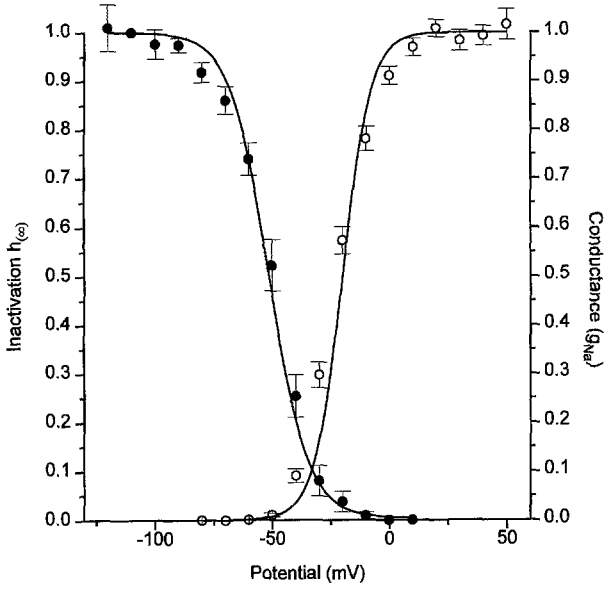

Fig. 8. The normalized mean conductance (○) and mean development of inactivation (●) are presented with standard error. On the left, steady state availability (or the h_∞ plot) is fit with a Boltzman distribution (n = 17 cells) with a half point at −51 mV and a steepness coefficient of 7.3 mV/e-fold. The steepness coefficient of the conductance curve was 5.3 mV/e-fold and the half-point was −22 mV. In the area of overlap, a steady Na "window" is present where some channels would be activated that would then not inactivate. The window of overlap occurs at approximately −33 mV where h_∞ = normalized $g_{(Na)}$ = 0.10.

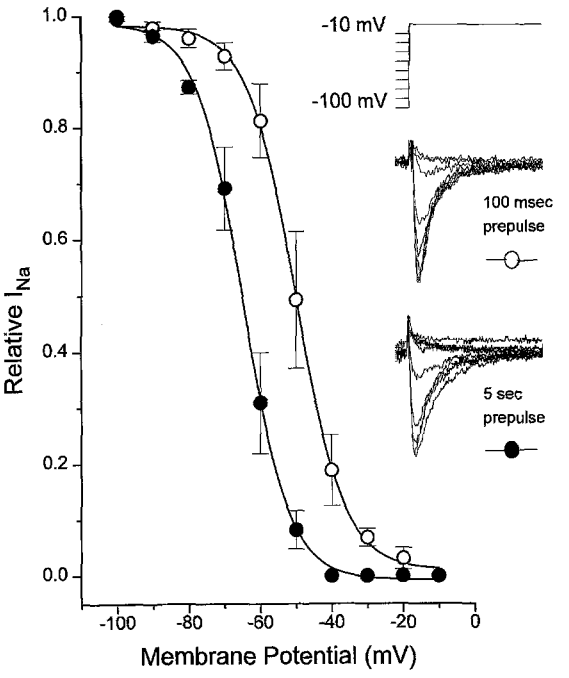

Fig. 9. In addition to fast inactivation, voltage-dependent sodium currents also displayed a slow inactivation. A prepulse potential, represented on the abscissa, was applied for either 100 msec (fast inactivation, ○, n = 4) or 5 seconds (slow inactivation, ●, n = 7) and then pulsed to the test potential of −10 mV. Slow inactivation resulted in a shift to the left of the voltage-dependence by approximately −15 mV. The half maximum potential for fast inactivation was −50 mV (steepness coefficient 6.7 mV/e-fold) compared to −65 mV (steepness coefficient 6.4 mV/e-fold) for slow inactivation.

constant was sought since the voltage-dependence is influenced by temporal parameters. For example, in using two identical voltage pulses from −80 to −10 mV, separated by variable time, *t*, held at the holding potential it was observed that as the interval between the pulses lengthened, the amount of sodium current generated by the second pulse gradually recovered to the control size of the first pulse. This recovery was approximately described by an exponential function, $[1 - \exp(t/\tau_h)]$. The time constant for inactivation at this potential was found to be close to 50 msec. This recovery (or removal) of inactivation was investigated at a series of membrane potentials and a series of durations as illustrated in Fig. 10*A*. Two identical 10 msec pulses, from a holding potential of −80 to −10 mV, were separated by varying durations (Δt) at either −50, −70, −90, −110, or −130 mV; this protocol is illustrated in the inset. A characteristic time constant could be generated at each test potential that described the recovery of inactivation at that potential. For potentials at and above −50 mV, where the removal of inactivation protocol could not be applied, the development of inactivation was studied. In this situation, cells were held at −80 mV, pulsed briefly to a prepulse (−50, −30, or −20 mV) and subsequently pulsed to −10 mV for 10 msec. This protocol was repeated with prepulses of varying durations. The development of inactivation could be measured as the amount of current inhibited compared to the first pulse. Each yielded a time constant for that particular prepulse as illustrated in Fig. 10*B*.

These time constants, τ_h, were found to be quite voltage dependent (Fig. 10*C*). Time constants derived from recovery from inactivation were plotted for test potentials in the range of −130 to −50 mV. Time constant values derived from the development of inactivation were plotted for values of −50 mV to −30 mV. For membrane potentials above −30 mV, time constants were taken from the inactivating current (Fig. 6). This voltage dependence of these time constants displayed a bell-shaped distribution with a maximum of 55 msec near the holding potential of −70 mV. On either side of this potential, the time constant diminished reaching a minimum of 10 msec at −130 mV, the most hyperpolarized test potential, and values below one millisecond at potentials more positive to −10 mV.

Tetrodotoxin Sensitivity of I_{Na}

Voltage-dependent sodium currents in dissociated taste receptor cells were reversibly inhibited by nanomolar

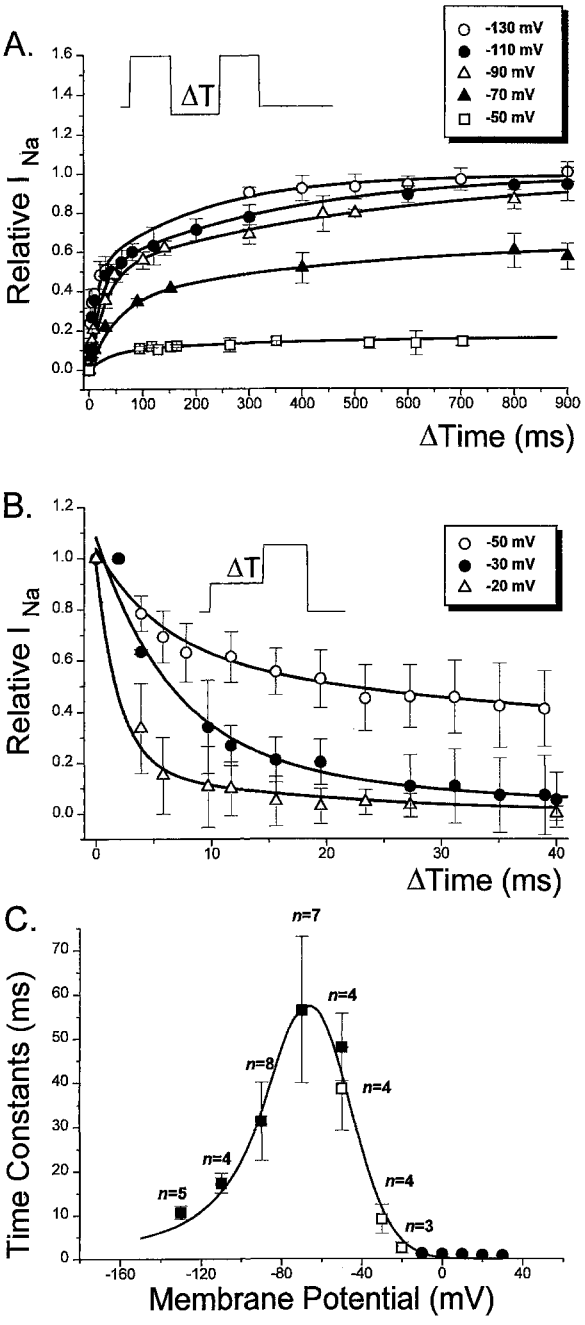

Fig. 10. Removal of inactivation (*A*) was tested with a two-pulse protocol where the first pulse that produced inactivation and the second pulse were separated by varying potentials for varying durations of time. Activation was measured as the amount of sodium current elicited by the second pulse relative to the amount of current elicited by the first pulse. In (*B*) the temporal development of inactivation was tested by pulsing the membrane potential, held at −80 mV, to one of three prepulse potentials (shown in inset) for varying durations depicted on abscissa. The amount of inactivation was assessed as the amount of current elicited by the second pulse to −10 mV relative to a pulse from −80 to −10 mV without the prepulse. In (*C*) the voltage-dependence of the time constant (τ) is plotted, producing a bell-shaped curve that peaked at −70 mV. Data were obtained from protocols for removal of inactivation (■), for development of inactivation (□), and from the decay of the inactivating sodium current (●). The fitted line represents a best fit using a Gaussian distribution with one peak.

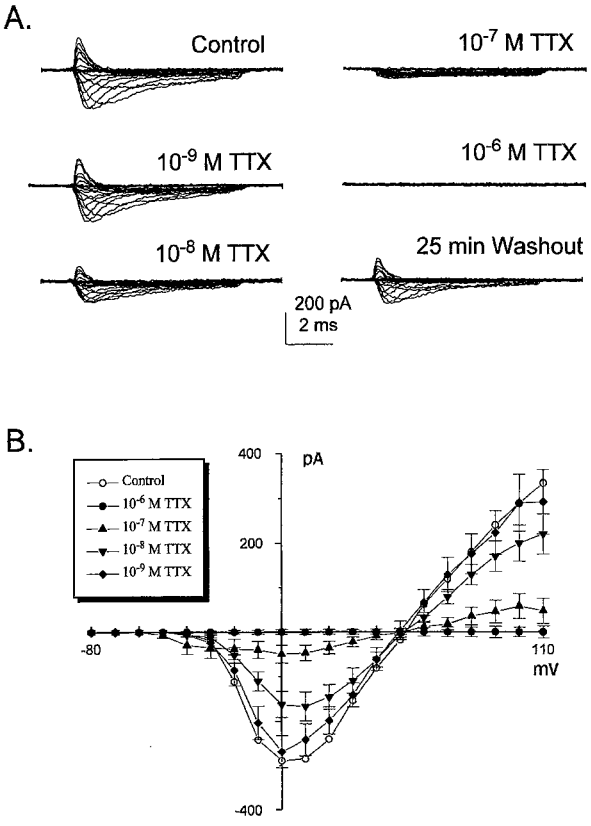

Fig. 11. The tetrodotoxin (TTX) sensitivity from a single taste cell to four sequential applications of TTX, applied in ascending order, is illustrated in (*A*). The current-voltage relationship for four concentrations of TTX is presented relative to pre-application values (labeled control in inset). Data are presented as mean ± SEM. Note that even the lowest concentration, 10^{-9} M TTX, produced some inhibition whereas none of the concentrations altered the reversal potential of the measured current.

concentrations of tetrodotoxin (TTX). Dose-response relationships were examined since TTX dose dependence in taste cells has not been reported. In all experiments, bath perfusion of TTX was held constant and always presented in ECF since TTX binding is strongly influenced by ionic strength as expected for a high field strength anionic site [17] and stimulus presentation rate [7, 12].

In Fig. 11*A*, data from one cell, tested with four concentrations of TTX, are presented. Currents were completely inhibited by TTX at 10^{-6} M and the inhibition was reversible when TTX was removed from the bath. In Fig. 11*B*, current-voltage relationships for the TTX-sensitive currents are presented for four concentrations of TTX. Data for each concentration are the mean of six to fourteen cells from a total of 41 cells. The current-voltage relationship of the TTX-sensitive current was entirely reminiscent of the sodium current. TTX did not alter the activation threshold, the voltage at which maximal peak I_{Na} was observed, or the reversal potential.

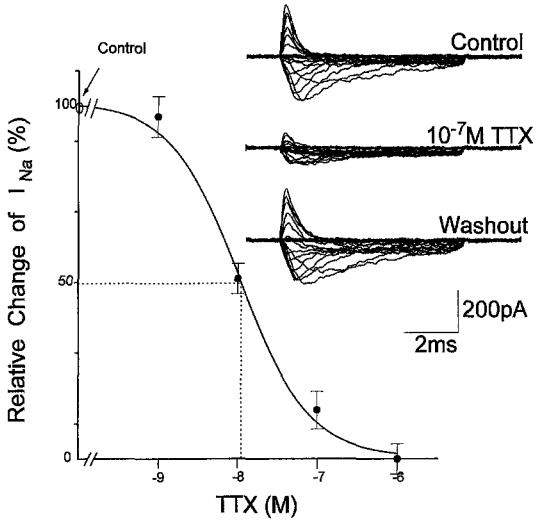

Fig. 12. The dose-response relationship of the inhibition of tetrodotoxin on sodium current is illustrated. The percent inhibition was calculated using a step potential from −80 to −10 mV before or during TTX application. Data are presented as the mean ± SEM from a total of 30 cells (minimum of three cells per point) and were fitted with a Boltzman distribution, illustrated as the solid line. Half-maximal inhibition was very close to 10^{-8} M TTX. The inset illustrates the reversibility of TTX inhibition by presenting a family of sodium currents from a single cell before, during, and after application of 10^{-7} M TTX.

TTX-sensitive currents at all concentrations reversed at an E_{rev} of +50 mV, as expected.

Figure 12 illustrates the dose-response curve for TTX (n = 30 cells). TTX reduced the current in a dose-dependent manner. This reduction in current was always reversible, as illustrated by current traces in the inset. The solid line was fitted to the data using a one-binding site model according to the equation:

$$\text{Relative } I_{Na} = \frac{1}{1 + ([TTX]/K_d)^n} \quad (4)$$

where $n = 1$. With this model, we obtained a K_d value very close to 10^{-8} M. Data were reasonably well described from the calculated curve and data fit was not improved if a two-binding site model ($n = 2$) was used.

Discussion

A thorough characterization of the behavior of voltage-dependent sodium currents is prerequisite to understanding the physiological role of the gustatory action potential. Knowledge of temporal and voltage-dependent characterizations, such as inactivation, allow prediction of a cell's ability or inability to fire action potentials under known physiological conditions. Voltage-dependent sodium currents were present in many, perhaps 50–75%, but not all taste receptor cells. The true percentage of taste cells possessing voltage-dependent sodium would provide an upper limit on the number of cells theoretically capable of contributing action potentials during physiological processing of gustatory stimuli. An accurate assessment of this value was not attempted in the present study. The absence of sodium currents cannot always be attributed to the lack of sodium channels since exogenous factors such as disruptive dissociation or poor clamping conditions may prevent their observation. For enigmatic reasons, in early recording sessions sodium currents were rarely observed in the majority of cells in which criteria for successful whole cell configuration were achieved. This observation is of interest when the wide range of this parameter in the few reports available on mammalian taste cells is considered. Although the majority of these reports agree with our present figure [9, 26, 38] one [1] places the percentage as low as 10%. Based on our recording experience, we now feel that these low ranges are not physiologically relevant.

Although many cell types appear to possess more than one type of sodium channel such as the squid axon [14, 29], frog node of Ranvier [11], sympathetic neurons [22], cardiac muscle [34], and skeletal muscle [13, 15, 16], the present data provide little indication of such heterogeneity of voltage-dependent sodium channel expression within taste cells. Electrophysiological properties were reasonably uniform in activation, inactivation, voltage-dependence, and pharmacology. Complexity did emerge, in comparison across cells, with magnitude of the peak inward current. This may be accounted for by a variation in sodium channel density across cells rather than multiplicity of channel type.

Variation of Sodium Channel Density Across Taste Cells

One possibility for the variation in maximal inward current recorded across taste cells (Fig. 4) is a variation in the sodium channel density. Whole-cell capacitance measures indicate that the size of dissociated taste cells was relatively consistent from cell to (Table; 3.69 ± 0.13 pF, n = 112 cells). Thus the distribution of maximal inward currents was maintained if expressed as current density. This conservatively implies that the variation in the magnitude of the peak inward sodium current could be a result of the number of functional sodium channels in the cell. For a conductance range of 6–10 nS (which accounts for the two peaks in Fig. 3), 400 to 600 μm^2 membrane surface area and an estimated single channel conductance of approximately 3–4 pS (Herness, *unpublished observation*) channel density would be 2 to 5 channels/μm^2. This density is reasonable for a nonpropagating excitable cell type such as a chromaffin cell (1–10 channels/μm^2, [19]).

Taste receptor cells undergo continual renewal, with a half life of approximately 10 days [10]. Little is known of how electrophysiological properties of taste receptor cells may fluctuate with cell age though correlations of channel density with either taste cell age or taste cell morphological type, though speculative, are intriguing.

The density could also vary if some channels were missed electrophysiologically. Sodium channels at the apical end of the cell could be up to 50 microns from electrode where a high access resistance and poor space clamp, such as with dendritic processes, might prevent adequate voltage clamp from the somatically located electrode. Our observations that sodium currents are more often recorded from cells with somatal swellings near the basolateral portion of the cell (rather than in the midregion of the cell) suggest this to be unlikely.

The Gustatory Action Potential

The physiological role of the gustatory action potential is uncertain. The usual explanation of taste cell action potentials is a rapid and complete depolarization of the taste cell allowing calcium to enter the cell and trigger transmitter release. One suggestion is that a regenerative event may be necessary to fully activate a low-threshold calcium current in these cells which is present in a low density [9].

Another unconsidered possibility is that the action potentials, in addition to serving as a signaling mechanism to the afferent nerve, may also serve to depolarize neighboring receptor cells through gap junctions. More evidence exists for gap junctions in lower vertebrates [40, 41] than in mammals [2, 20]. Only a minority of taste receptor cells make synapticlike contacts with neural elements [e.g., 25, 32, 35]. The type III cell possess the clearest examples of synapticlike structures with electron-dense cored vesicles, interspersed with clear vesicles. These cells are most often discussed as true "receptor" cells. However, they make up only 5–15% of the entire bud. Type II cells also make synapticlike structures with neural elements, though only clear vesicles are present but are more often discussed as efferent than afferent. These constitute another 15–30% of the cells. Type I cells, the most prevalent at 55–75%, do not make synaptic contacts and are thought of as supportive because of irregular cytoplasmic processes which in thin lamella surround type II and type III cells. If 50–75% of cells possess voltage-dependent sodium currents then it is numerically possible that some type I cells could conduct action potentials. Presently, there are no data to suggest that type I cells, though of similar morphology, are homogeneous in electrophysiological properties. However, the possibility remains that taste receptor cells without synaptic neural connections may conduct action potentials and that some information processing may occur within the mammalian taste bud from taste cell to taste cell.

Sodium Current Inactivation and Afferent Firing Rate

Many details of how action potentials in taste cells initiate action potentials in the afferent nerve fiber remain to be elucidated. For example, it is not known how many sensory afferent impulses might be produced by a single impulse in the taste receptor cell. Inactivation time constants of taste cell sodium currents are slow when compared to neurons. A maximal time constant on the order of 55 msec occurred at −70 mV. Thus when the membrane potential returned to a resting level after firing an action potential, several decades of milliseconds must pass before a sufficient number of sodium channels would be available to fire another impulse. This agrees quite well with the observation that taste cells stimulated with strong stimuli fired at 6 to 10 Hz [6]. The firing rate of a gustatory afferent, however, can approach 100 Hz [37]. These differences are not incompatible if the ratio of action potentials in taste receptor cells to that of its sensory afferent is less than unity. Several factors may contribute. A single receptor cell action potential could release sufficient transmitter to produce multiple action potentials in the afferent nerve. Additionally many taste receptor cells may contribute to afferent impulses. In the rat, a single gustatory chorda tympani afferent innervates several taste buds as well as several cells within the bud. Isolated stimulation of any of the individual taste buds which a single afferent fiber innervates results in a series of impulses in that fiber [30, 31]. Hence this convergence would permit many receptor cells to contribute to the firing rate of a single gustatory afferent fiber.

This work was supported by National Institutes of Health grant NIDCD DC00401.

References

1. Akabas, M.H., Dodd, J., Al-Awqati, Q. 1990. Identification of electrophysiologically distinct subpopulations of rat taste cells. *J. Membrane Biol.* **114:**71–78
2. Akisata, T., Oda, M. 1978. Taste buds in the vallate papillae of the rat studied with freeze-fracture preparation. *Arch. Histol. Jpn.* **41:**87–98
3. Almers, W. 1978. Gating currents and charge movements in excitable membranes. *Rev. Physiol. Biochem. Pharmacol.* **82:**96–190
4. Almers, W., Roberts, W.M., Ruff, R.L. 1984. Voltage clamp of rat and human skeletal muscle: Measurements with an improved loose-patch technique. *J. Physiol.* **347:**751–768
5. Avenet, P., Lindemann, B. 1987. Patch-clamp study of isolated taste receptor cells of the frog. *J. Membrane Biol.* **97:**223–240
6. Avenet, P., Lindemann, B. 1991. Noninvasive recording of receptor cell action potentials and sustained currents from single taste

buds maintained in the tongue: The response to mucosal NaCl and amiloride. *J. Membrane Biol.* **124:**33–41
7. Baer, M., Best, P.M., Reuter, H. 1976. Voltage-dependent action of tetrodotoxin in mammalian cardiac muscle. *Nature* **263:**344–345
8. Barres, B.A., Chun, L.L.Y., Corey, D.P. 1989. Glial and neuronal forms of the voltage-dependent sodium channel: Characteristics and cell-type distribution. *Neuron* **2:**1375–1388
9. Béhé, P., DeSimone, J.A., Avenet, P., Lindemann, B. 1990. Membrane currents in taste cells of the rat fungiform papilla. Evidence for two types of Ca currents and inhibition of K currents by saccharin. *J. Gen. Physiol.* **96:**1061–1084
10. Beidler, L.M., Smallman, R.L. 1965. Renewal of cells within taste buds. *J. Cell Biol.* **27:**263–272
11. Benoit, E., Corbier, A., Dubois, J.M. 1985. Evidence for two transient sodium currents in the frog node of Ranvier. *J. Physiol.* **361:**339–360
12. Cohen, C.J., Beam, B.P., Colatsky, T.J., Tsien, R.W. 1981. Tetrodotoxin block of sodium channels in rabbit Purkinje fibers: Interactions between toxin binding and channel gating. *J. Gen. Physiol.* **78:**383–411
13. Frelin, C., Vigne, P., Lazdunski, M. 1983. Na^+ channels with high and low affinity tetrodotoxin binding sites in the mammalian skeletal muscle cell. Difference in functional properties and sequential appearance during rat skeletal myogenesis. *J. Biol. Chem.* **258:** 7256–7259
14. Gilly, W.F., Armstrong, C.M. 1984. Threshold channels—novel type of sodium channel in squid giant axon. *Nature* **309:**448–450
15. Gonoi, T., Sherman, S.J., Catterall, W.A. 1985. Voltage clamp analysis of tetrodotoxin-sensitive and -insensitive sodium channels in rat muscle cells developing in vitro. *J. Neurosci.* **5:**2559–2564
16. Haimovich, B., Tanaka, J.C., Barchi, R.L. 1986. Developmental appearance of sodium channel subtypes in rat skeletal muscle cultures. *J. Neurochem.* **47:**1148–1152
17. Henderson, R., Ritchie, J.M., Strichartz, G.R. 1974. Evidence that tetrodotoxin and saxitoxin act at a metal cation binding site in the sodium channels of nerve membrane. *Proc. Nat. Acad. Sci. USA* **71:**3936–3940
18. Herness, M.S. 1989. A dissociation procedure for mammalian taste cells. *Neurosci. Lett.* **106:**60–64
19. Hille, B. 1992. Ionic channels in excitable membranes. Sinauer, Sunderland, MA
20. Holland, V.F., Zampighi, G.A., Simon, S.A. 1989. Morphology of fungiform papillae in canine lingual epithelium: Location of intercellular junctions in the epithelium. *J. Comp. Neurol.* **279:**13–27
21. Howe, J.R., Ritchie, J.M. 1990. Sodium currents in Schwann cells from myelinated and non-myelinated nerves of neonatal and adult rabbits. *J. Physiol.* **425:**169–210
22. Jones, S.W. 1987. Sodium currents in dissociated bull-frog sympathetic neurones. *J. Physiol.* **389:**605–627
23. Kashiwayanagi, M., Miyake, M., Kurihara, K. 1983. Voltage-dependent Ca^{+2} channel and Na^+ channel in frog taste cells. *Am. J. Physiol.* **244:**C82–88.
24. Keynes, R., Rojas, E. 1976. The temporal and steady-state relationships between activation of the sodium conductance and movement of the gating particles in the squid giant axon. *J. Physiol.* **255:**157–189
25. Kinnamon, J.C. 1986. Organization and Innervation of Taste Buds. *In:* Neurobiology of Taste and Smell, Chap. 12, T.E. Finger and W.L. Silver, editors, pp. 277–297. John Wiley & Sons, New York
26. Kinnamon, S.C., Cummings, T.A. 1992. Chemosensory transduction mechanisms in taste. *Ann. Rev. Physiol.* **54:**715–731
27. Kinnamon, S.C., Roper, S.D. 1988. Membrane properties of isolated mudpuppy taste cells. *J. Gen. Physiol.* **91:**351–371
28. Marty, A., Neher, E. 1983. Tight-seal whole-cell recording. *In:* Single-Channel Recording, B. Sakmann, & E. Neher, editors, pp. 107–122. Plenum, New York
29. Matteson, D.R., Armstrong, C.M. 1982. Evidence for a population of sleepy sodium channels in squid axon at low temperature. *J. Gen. Physiol.* **79:**739–758
30. Miller, I.J. 1971. Peripheral interactions among single papilla inputs to gustatory nerve fibers. *J. Gen. Physiol.* **57:**1–25
31. Miller, I.J. 1974. Branched chorda tympani neurons and interactions among taste receptors. *J. Comp. Neurol.* **158:**155–156
32. Murray, R.G. 1986. The mammalian taste bud type III cell: a critical analysis. *J. Ultrastrct. Molec. Struct. Res.* **95:**175–188
33. Pappone, P.A. 1980. Voltage-clamp experiments in normal and denervated mammalian skeletal muscle fibers. *J. Physiol.* **306:** 377–410
34. Patlak, J., Ortizm, M. 1985. Slow currents through single sodium channels of the adult rat heart. *J. Gen. Physiol.* **86:**89–104
35. Reutter, K., Witt, M. 1993. Morphology of vertebrate taste organs and their nerve supply. *In:* Mechanisms of Taste Transduction, Chap. 2, S.A. Simon and S.D. Roper, editors, pp. 29–82. CRC, Boca Raton
36. Roper, S.D. 1983. Regenerative impulses in taste cells. *Science* **220:**1311–1312
37. Smith, D.V., Bealer, S.L. 1975. Sensitivity of the rat gustatory system to the rate of stimulus onset. *Physiol. & Beh.* **15:**303–314
38. Spielman, A.I., Mody, I., Brand, J.G., Whitney, G., MacDonald, J.F., Salter, M.W. 1989. A method for isolating and patch clamping single mammalian taste receptor cells. *Brain Res.* **503:**326–329
39. Stühmer, W., Methfessel, C., Sakmann, B., Noda, M., Numa, S. 1987. Patch-clamp characterization of sodium channels expressed from rat brain cDNA. *Euro. Biophys. J.* **14:**131–138
40. Teeter, J. 1985. Dye-coupling in catfish taste buds. *In:* Proceedings of the 19th Japanese Symposium on Taste and Smell, K. Ueda, editor, pp. 29–33. JASTS, Osaka, Japan
41. Yang, J., Roper, S. 1987. Dye-coupling in taste buds in the mudpuppy *Necturus maculosus. J. Neurosci.* **7:**3561–3565